Search for parity violation in deep-inelastic scattering of polarized electrons by unpolarized deuterons

W. B. Atwood, R. L. A. Cottrell, H. DeStaebler, R. Miller, H. Pessard,* C. Y. Prescott, L. S. Rochester, and R. E. Taylor
Stanford Linear Accelerator Center, Stanford University, Stanford, California 94305

M. J. Alguard, J. Clendenin, P. S. Cooper, R. D. Ehrlich,† V. W. Hughes, and M. S. Lubell
Yale University, New Haven, Connecticut 06520

G. Baum and K. P. Schüler
University of Bielefeld, Bielefeld, West Germany

K. Lübelsmeyer
Technische Hochschule Aachen, Aachen, West Germany

(Received 17 April 1978)

We report on recent asymmetry measurements for inelastic scattering of longitudinally polarized electrons from an unpolarized deuterium target at 19.4 GeV. Using the SLAC 20-GeV/c and 8-GeV/c spectrometers, the helicity-dependent cross-section asymmetries were measured at Q^2 values of 1.2 and 4.2 $(\mathrm{GeV}/c)^2$, and were found to be less than 2×10^{-3} and 7×10^{-3}, respectively.

The motivation for searching for parity-violating effects in electromagnetic interactions has come primarily from interest in the ideas which unify the weak and electromagnetic forces. The experimental discovery of neutral-current events in neutrino experiments intensified the interest in gauge theories and their consequences, including the possibility of parity-violating effects in the electromagnetic interactions. In the case of inelastic electron scattering, parity violation can show up as a helicity dependence of the differential cross section for a longitudinally polarized beam of electrons scattering from an unpolarized target.[1,2,3] We report here on an experiment undertaken to improve limits for parity-violating terms in inelastic scattering of longitudinally polarized electrons from an unpolarized deuterium target at an incident energy of 19.4 GeV using two spectrometers set at the kinematic points given in Table I.

The helicity-dependent cross section may be written

$$d\sigma^{(\lambda)} = d\sigma_0(1+\lambda P_e A)\,, \tag{1}$$

in which $\lambda(=\pm1)$ is the helicity of the incident electron beam, $d\sigma_0$ is the differential cross section for an unpolarized beam, P_e is the magnitude of the polarization, and A is the asymmetry

$$A = \frac{1}{P_e}\,\frac{d\sigma^+ - d\sigma^-}{d\sigma^+ + d\sigma^-}\,. \tag{2}$$

All theoretical models agree that A is proportional to Q^2, the four-momentum transfer squared in the scattering, but predictions[4,5,6] of the size of A vary widely but are generally in the range of $|A| \simeq (10^{-5}$ to $10^{-4})\times[Q^2\ (\mathrm{GeV}/c)^2]$. Previous experiments have reported the following limits on A at the 95% confidence level for elastic e-p and deep-inelastic e-nucleon[7] and μ-nucleon[8] scattering: $|A|<3\times10^{-3}$ for elastic e-p scattering at $Q^2=0.765$ $(\mathrm{GeV}/c)^2$, $|A|<3\times10^{-3}$ for deep-inelastic e-nucleon scattering for Q^2 between 1 and 4 $(\mathrm{GeV}/c)^2$, and $|A|<1.6\times10^{-2}\times[Q^2\ (\mathrm{GeV}/c)^2]$ for deep-inelastic muon-nucleon scattering for Q^2 between 1 and 10 $(\mathrm{GeV}/c)^2$. Our present experiment emphasizes the careful study of systematic errors and is considered as the first step toward a still higher sensitivity measurement of A at the level predicted by modern gauge theories.

Polarized electrons were provided by the Yale-SLAC polarized-electron source (PEGGY),[9] which is based on photoionization of a polarized Li^6 atomic beam by a pulsed uv light source.[10] Typical operation yielded 1.2×10^9 electrons per pulse. Longitudinally polarized electrons were accelerated in the linear accelerator with negligible depolarization, as confirmed by earlier tests.[11] The electron polarization P_e was measured frequently during the experiment by Mott scattering at the output of PEGGY, and at the beginning and end of the experiment by electron-electron (Møller) scattering at high energy. For Møller scattering a thin magnetized Supermendur foil was placed in the beam and elastically scattered electrons with one half the beam energy, corresponding to symmetric 90° scattering in the e-e c.m.-system frame, were detected in the 20-GeV/c spectrometer. PEGGY was operated in a mode to

TABLE I. Kinematic points.

	20-GeV/c spectrometer	8-GeV/c spectrometer
Laboratory angle (deg)	3.5	13.3
Scattered energy E' (GeV)	16.5	4.0
Q^2 [(GeV/c)^2]	1.2	4.2
Missing mass W (GeV)	2.3	5.1
$\nu = E_0 - E'$ (GeV)	2.9	15.4
$\omega = 2M\nu/Q^2$	4.5	6.9
$x = 1/\omega$	0.22	0.15
$y = \nu/E_0$	0.15	0.79

increase available beam intensity which, due to a two-step photoionization process, reduced the polarization to $P_e = 45 \pm 6\%$.[12] The helicity of the PEGGY beam is determined by the direction of a static magnetic field of about 200 G in the photoionization region, and this field direction could be reversed in a period of a few seconds.

The target was a 30-cm-long cell of liquid deuterium. The liquid deuterium target was chosen over one of liquid hydrogen primarily because of increased yields of electrons. The 8- and 20-GeV/c spectrometers were used in a manner similar to previous inelastic electron experiments at SLAC.[13]

Experimental sensitivity to parity-violating effects depends on many parameters including kinematical variables, the electroproduction cross-section values, and spectrometer acceptance. If we define sensitivity to be the ratio $A/\Delta A$, take A to be linear in Q^2, and calculate ΔA from counting statistics, we find that higher Q^2 points yield lower sensitivity. Having chosen kinematical points at low Q^2 to enhance the statistical accuracy, we must then control and measure small systematic effects arising from drifts in the beam parameters, as well as from changes in beam parameters that may be associated with reversal of the polarization. Unobserved systematic changes can mask or create apparent parity-violating effects. Beam parameters on which the yield of scattered electrons depends were monitored, including beam position on target, angle of beam on target, beam current, and beam energy. The instrumentation of the beam line is shown schematically in Fig. 1.

Beam positions were measured using nonintercepting resonant microwave cavities which were installed at two points along the beam before the target, positioned such that cavity nodes fall on the beam axis. For small displacements of the beam off the axis, signals were induced in an amount proportional to the product of the beam current times its transverse displacement.[14] Beam currents were separately measured, so that the displacements could be calculated. The positions, averaged over the 1.5-μsec duration of the beam pulse, were measured at two points in the horizontal and two points in the vertical direction. Sensitivity, limited only by electronic noise, was good to a few microns displacement. Drifts in position and angle were sensed by a computer, and steering corrections were applied automatically by adjusting currents in the beam-line magnets. With automatic computer steering in use, syste-

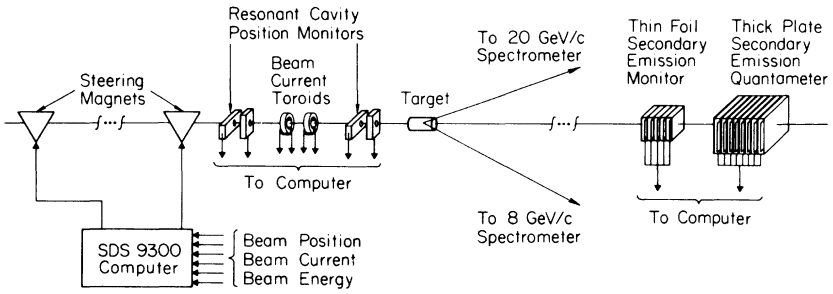

FIG. 1. Beam-line instrumentation, shown schematically (not to scale), installed to monitor and control beam position, angle, intensity, and energy changes that may be associated with polarization reversals. Spectrometers are not shown. Computer steered position and angle of beam on target with separate horizontal and vertical adjustments on beam-magnet currents.

matic position changes between opposite-helicity beams were held to less than 1 μm, and systematic angle changes for the beam at the target were held to less than 0.1 μrad.

Beam currents were measured with two independent nonintercepting beam toroids. The digitized toroid signals provided a measurement of beam flux to an absolute accuracy of 1%. Imbalances in the beam currents can generate systematic errors through electronic dead times and nonlinearities. Averaged over this experiment the opposite-helicity beam currents were balanced to 0.1%. Errors introduced in the measured asymmetries were estimated and separately measured to be negligible.

Downstream from the target, intercepting the beam, we placed a thin foil secondary emission monitor followed by a thick plate secondary emission quantameter. The induced secondary emission currents were proportional to the beam current I in the monitor and to IE_0 in the quantameter. The outputs of these, digitized for each beam pulse, and their ratio provided a signal proportional to the beam energy E_0.

Data were taken in sets of eight minirums with each minirun approximately 1 minute in length. Cross-section values were measured for each minirun. Every two miniruns the beam polarization was reversed and successive sets of eight miniruns had the overall sign of the polarization reversed, giving a helicity pattern:

$$\cdots(++--+--),(--++--++),\cdots.$$

From the cross-section values of each set we construct the asymmetry A of Eq. (2) and a number of false asymmetries (37, but not all independent). The false asymmetries serve to identify transient or cyclic effects correlated with the pattern and also provide a measure of the systematic and statistical noise. The data-taking time was about 100 hours with a pulse rate of 120 pulses per sec.

From each set of eight miniruns we calculate the asymmetry A, the statistical error ΔA, and take the ratio $A/\Delta A$. In Fig. 2 we show the distributions of $A/\Delta A$ for all sets of eight miniruns, and superimpose on them normal curves expected for purely statistical errors. The distributions agree well with the expected curve and no asymmetries lie outside 3.5 standard deviations. In Fig. 3 we show the distribution of false asymmetries and one real asymmetry, for each kinematical point. Separately shown in Fig. 3 are systematic errors which were estimated as follows. We looked for changes in beam angle and position on the target, average current, and beam energy correlated with reversal of polarization. Only in the case of beam energy was there a significant effect, where an apparent asymmetry of 6×10^{-5}, corresponding to an average energy difference of 2.3 MeV between the two beams of opposite helicity, was seen. Such an effect could arise from small movements of the beam where it passes through energy-defining slits in the beam transport system, when helicity is reversed. We calculate the effect on our measured cross sections

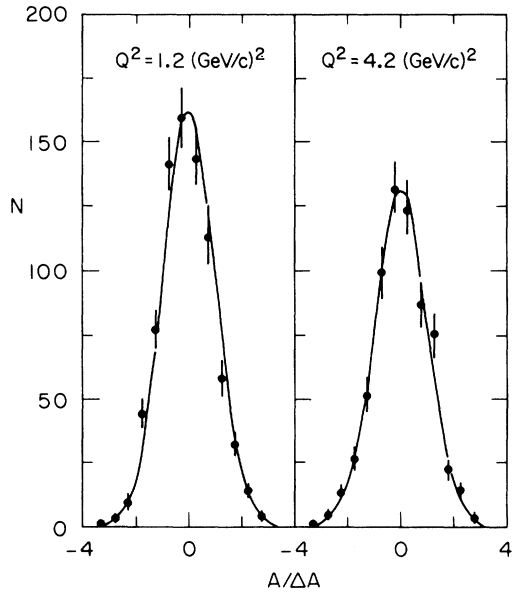

FIG. 2. Distributions for set-of-eight-miniruns asymmetries, A, divided by the statistical error, ΔA, for the two kinematic points, $Q^2 = 1.2$ (GeV/c)^2 and $Q^2 = 4.2$ (GeV/c)^2. The solid curves are normal distributions with zero mean and unit standard deviation. No asymmetries lie outside 3.5 standard deviations from zero. The distributions agree with the curves although for the low-Q^2 point the mean of the distribution is slightly negative.

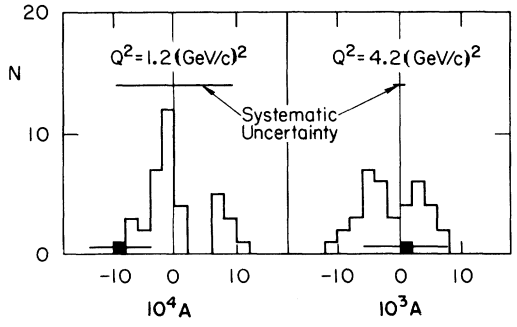

FIG. 3. Asymmetry A (black square) averaged over all sets of eight miniruns and distribution of false asymmetries for the two kinematic points $Q^2 = 1.2$ (GeV/c)^2 and $Q^2 = 4.2$ (GeV/c)^2. Statistical error for A is shown. Systematic uncertainties are separately shown as error bars centered at 0.

and consider this uncertainty as our systematic error. The asymmetries we obtain, with statistical (1 standard deviation) and systematic errors respectively, are

$$Q^2 = 1.2\ (\mathrm{GeV}/c)^2\text{:}\quad A = (-8.2 \pm 4.4 \pm 9.3)\times 10^{-4},$$
$$Q^2 = 4.2\ (\mathrm{GeV}/c)^2\text{:}\quad A = (0.44 \pm 6.9 \pm 0.42)\times 10^{-3}. \tag{3}$$

We assume that the asymmetry will have a form linear in Q^2. With M the nucleon mass we take

$$A = g\,Q^2/M^2. \tag{4}$$

Then if we add (linearly) the systematic errors to the statistical errors and form the weighted average of our two data points, we obtain

$$g = (-3.9 \pm 8.4)\times 10^{-4}.$$

We note that a conventional $V-A$ weak interaction interfering with the electromagnetic interaction leads to a prediction $g \cong -2\times 10^{-4}$ and the Weinberg-Salam SU(2)×U(1) unified gauge theory predicts $g \simeq -(3 \text{ to } 9)\times 10^{-5}$ for $\sin^2\theta_W = 0.33$ to 0.20, $Q^2 = 1.2\ (\mathrm{GeV}/c)^2$, and $y = 0.15$. Both of these are smaller than our present errors.

Another experiment with a much more intense polarized electron source[15] based on photoemission from Ga-As and with much improved control of systematic errors is in progress.

Note added in proof. Results from this more sensitive experiment have recently been published by C. Y. Prescott *et al.*, Phys. Lett. 77B, 347 (1978).

We wish to acknowledge the important contributions to this experiment by M. Browne, R. Eisele, Z. Farkas, H. Hogg, and H. Martin. This work was supported in part by the U.S. Department of Energy.

---

*Present address: Annecy (LAPP), 74019 Annecy-le-Vieux, France.
†Present address: Cornell University, Ithaca, NY 14850.

[1]E. Derman, Phys. Rev. D 7, 2755 (1973).
[2]W. J. Wilson, Phys. Rev. D 10, 218 (1974).
[3]S. M. Berman and J. R. Primack, Phys. Rev. D 9, 2171 (1974); 10, 3895 (E) (1974).
[4]M. A. B. Bég and G. Feinberg, Phys. Rev. Lett. 33, 606 (1974).
[5]S. M. Bilenkii *et al.*, Yad. Fiz. 21, 1271 (1975) [Sov. J. Nucl. Phys. 21, 657 (1975)].
[6]R. N. Cahn and F. J. Gilman, Phys. Rev. D 17, 1313 (1978).
[7]M. J. Alguard *et al.*, Phys. Rev. Lett. 37, 1258 (1976); 37, 1261 (1976); *ibid.* 41, 70 (1978).
[8]Y. B. Bushnin *et al.*, Yad. Fiz. 24, 536 (1976) [Sov. J. Nucl. Phys. 24, 279 (1976)].
[9]M. J. Alguard *et al.*, in *Proceedings of the IXth International Conference on High Energy Accelerators, 1974* (Stanford Linear Accelerator Center, Stanford, Cal; 1974), p. 309.
[10]V. W. Hughes *et al.*, Phys. Rev. A 5, 195 (1972).
[11]P. S. Cooper *et al.*, Phys. Rev. Lett. 34, 1589 (1977).
[12]M. J. Alguard *et al.*, Phys. Rev. A 16, 209 (1977).
[13]S. Stein *et al.*, Phys. Rev. D 12, 1884 (1975) and references therein.
[14]Z. D. Farkas *et al.*, SLAC Report No. SLAC-PUB-1823, 1976 (unpublished).
[15]C. K. Sinclair *et al.*, in *High Energy Physics with Polarized Beams and Targets*, proceedings of the Argonne Symposium, edited by M. L. Marshak (AIP, New York, 1976), p. 424.

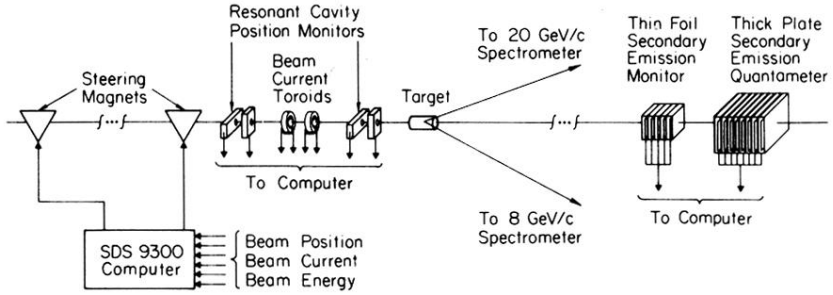

FIG. 1. Beam-line instrumentation, shown schematically (not to scale), installed to monitor and control beam position, angle, intensity, and energy changes that may be associated with polarization reversals. Spectrometers are not shown. Computer steered position and angle of beam on target with separate horizontal and vertical adjustments on beam-magnet currents.

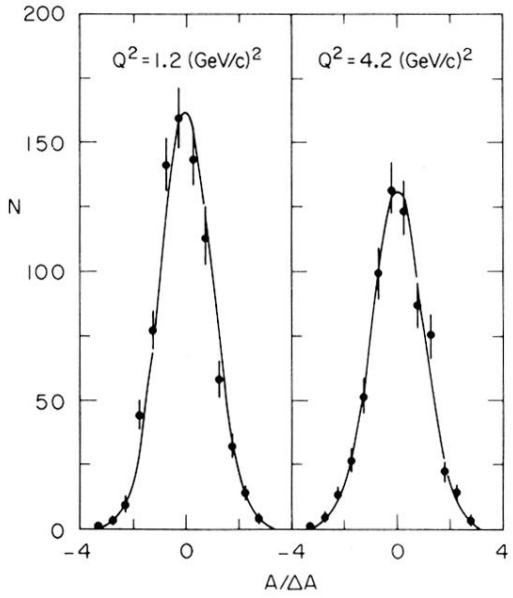

FIG. 2. Distributions for set-of-eight-miniruns asymmetries, A, divided by the statistical error, ΔA, for the two kinematic points, $Q^2 = 1.2$ (GeV/c)^2 and $Q^2 = 4.2$ (GeV/c)^2. The solid curves are normal distributions with zero mean and unit standard deviation. No asymmetries lie outside 3.5 standard deviations from zero. The distributions agree with the curves although for the low-Q^2 point the mean of the distribution is slightly negative.

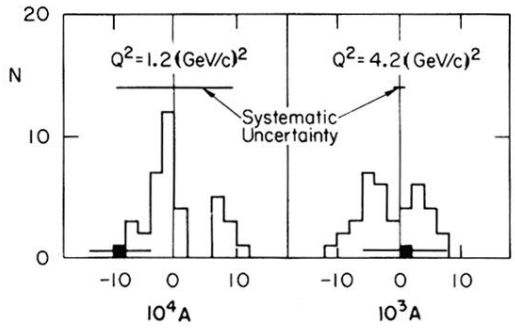

FIG. 3. Asymmetry A (black square) averaged over all sets of eight miniruns and distribution of false asymmetries for the two kinematic points $Q^2 = 1.2$ (GeV/c)^2 and $Q^2 = 4.2$ (GeV/c)^2. Statistical error for A is shown. Systematic uncertainties are separately shown as error bars centered at 0.